4. *In silico* studies

According to the literature survey, various anti-AD scaffolds including pyrazole, benzyl piperidine, carbamate, benzofuran, vicinal diaryl and urea derivatives have been reported and discussed in the literature review chapter. With an aim to design novel compounds using above mentioned chemical scaffolds, *in silico* studies were caried out. Molecular docking was caried out for the combination of various scaffolds for more than thousands of compounds to check its affinity and prioritize against AChE, BuChE and MAO-B enzyme. Considering highest docking affinity score, interaction and orientation of designed compounds, the most appropriate series of compounds (**Table 4.1**) were designed and considered for further development as anti-AD agents and most potent (**D1-D13**) are discussed.

Table 4.1: Designing of molecules via combination of scaffolds.

Derivative	Structure	Remark
Vicinal diaryl pyrazole fused benzyl piperidine derivatives **(I)**	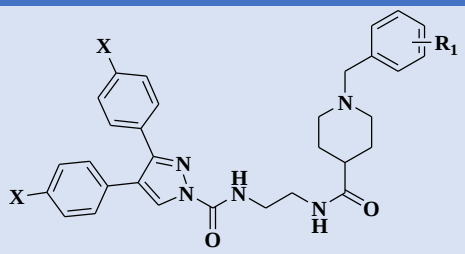	**X**= H, OCH_3, Cl **R_1**= H, Cl, diCl, CF_3, OCH_3, CH_3, NO_2
Vicinal diaryl pyrazole fused carbamate derivatives **(II)**	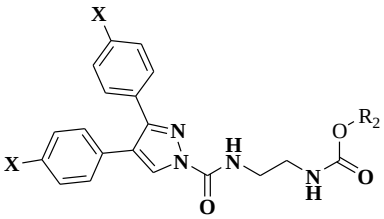	**X**= H, OCH_3, Cl **R_2** = Phenyl, Isobutyl, Ethyl, Methyl, n-Pentyl, Benzyl, 2,2,2-Trichloroethyl, 9*(H)* Fluorenyl methyl
Benzofuran fused carbohydrazide derivatives **(III)**	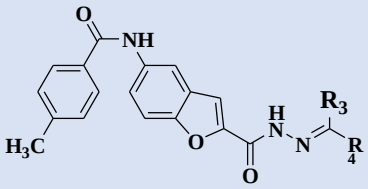	**R_3=** H, CH_3, Benzyl **R_4** = Aromatic, Aliphatic, Heterocyclic.

Benzofuran fused carbamate and amide derivatives **(IV)**	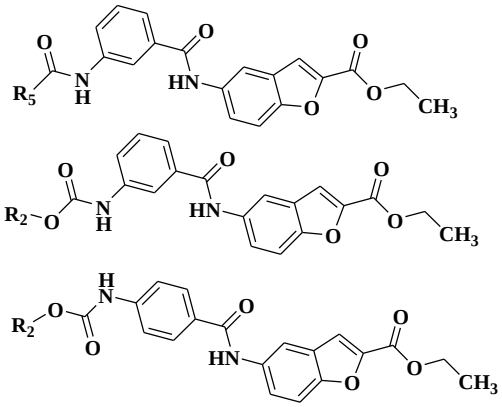	**R_2** = Phenyl, Isobutyl, Ethyl, Methyl, n-Pentyl, Benzyl, 2,2,2-Trichloroethyl, 9*(H)* fluorenyl methyl **R_5** = Benzyl, Phenylacetyl, Isonicotinyl, Napthyl, Chloroacetyl.

The molecular docking study has been discussed as follows:

4.1. *In silico* studies of vicinal diaryl pyrazole-based compounds

4.2. *In silico* studies of benzofuran based compounds

4.1. *In silico* studies of vicinal diaryl pyrazole-based compounds

All the designed compounds were docked and analysed by the binding energies and receptor ligand interactions. The interactions of designed compounds (**D1- D6)** respectively within active site of *h*AChE, BuChE and MAO-B are discussed in **Table 4.2.**

Table 4.2: Docking score and interactions of **D1-D6** against *h*AChE (PDB: 4EY7), *h*BuChE (PDB: 5K5E), *h*MAO-B (PDB: 2V5Z).

Code	Compound	*h*AChE (PDB: 4EY7)		*h*BuChE (PDB: 5K5E)		*h*MAO-B (PDB: 2V5Z)	
		Docking Score (Kcal/Mol)	Interaction	Docking Score (Kcal/Mol)	Interaction	Docking Score (Kcal/Mol)	Interaction
D1	**96**	-12.018	Trp86 Tyr337 Phe295 Trp286	-6.871	Trp82	-10.099	Ile199 Trp388 Tyr396
D2	**111**	-10.206	Asn74 Phe295 Tyr341 Tyr337 His447	-8.029	Ser287 Phe329	-11.852	Tyr326 Gln206 Trp388
D3	**121**	-12.418	Trp86 Phe295 Trp286	-8.716	Trp82 His438	-10.552	Leu171 Tyr398 Tyr435

			Tyr337				
D4	**136**	-8.78	Trp86 Trp286	-7.12	Trp82 Ser287 Phe329 His438	-9.498	Gln206
D5	**132**	-7.678	Tyr72 Phe295 Trp286	-6.923	Trp82 Phe329 Tyr332 His438	-6.359	Tyr188 Lys296 Phe343 Tyr398
D6	**152**	-9.078	Trp86 Trp286 Ser293	-7.169	Phe329 Tyr332	-6.697	Gln206 Tyr398 Met436

Grid validation was performed by redocking of co-crystalized molecules in 3D protein structures of *h*AChE (**PDB: 4EY7**), *h*BuChE (**PDB: 5K5E**) and *h*MAO-B (**PDB: 2V5Z**) active site. Initially, co-crystallized ligands were extracted from the binding site. This extracted co-crystalized ligand were energy minimized and redocked into the active site. **Fig. 4.1** has shown the RMSD value of redocked ligands with co-crystallized ligands in 4EY7, 5K5E and 2V5Z were observed which were 0.14 (**Fig. 4.1A**), 1.37 (**Fig. 4.1B**) and 0.53 (**Fig. 4.1C**), respectively.

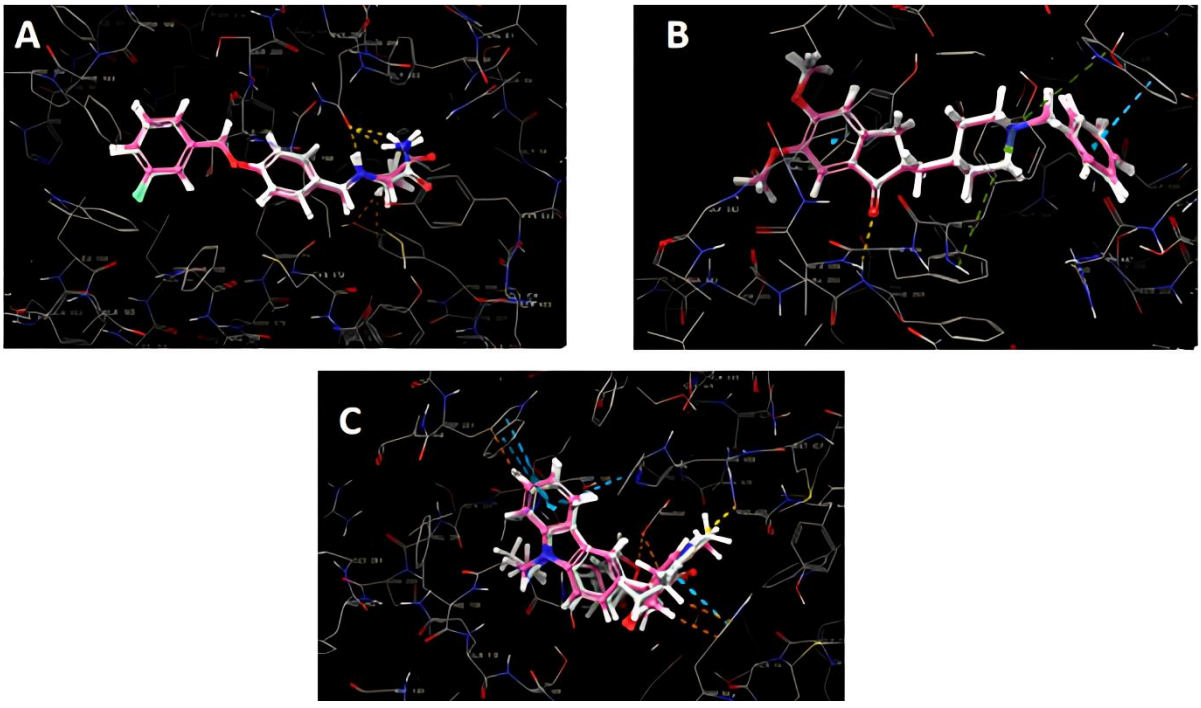

Fig. 4.1: Aligned redocked ligands (pink) with co-crystallized ligand (white) for 2V5Z (A), 4EY7 (B) and 5K5E (C).

The bipartite MAO-B active site consists of two cavities: an entry cavity and a substrate cavity with an aromatic cage[1]. Active compounds **D1-D6** entered into the active site of MAO-B and interacted with its amino acids. They interacted with Pro102, Ile199 and

Tyr326 which are key amino acids of entrance cavity, besides that they also interacted with substrate cavity key amino acids such as Phe343, Trp388, Tyr398, Tyr435 and Met436.

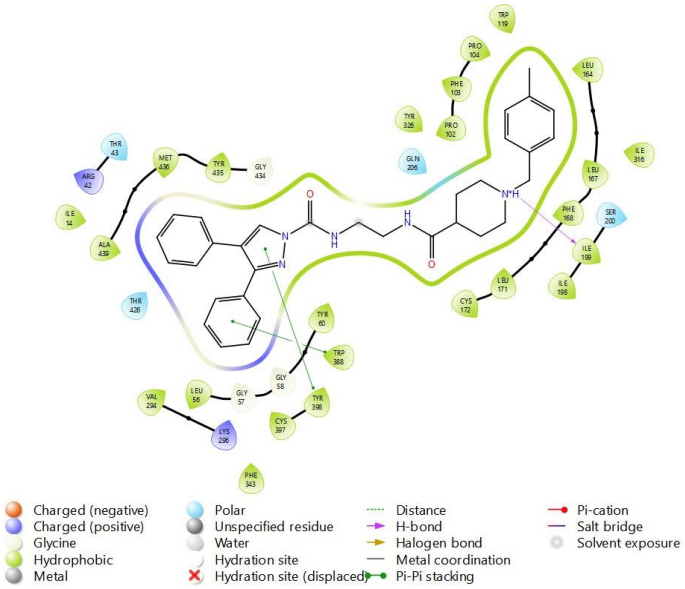

Fig. 4.2: 2D interactions of compound **D1** with MAO-B (PDB Id- 2V5Z).

Fig. 4.2. shows the interaction of compound **D1** with active site of MAO-B. NH of benzyl piperidine interacted with bridge of the substrate cavity amino acid Tyr326 via H-bond interaction and vicinal diaryl pyrazole moiety entered in the substrate site and interacted with and phenyl ring interacted with amino acid Trp388 and Tyr398 of aromatic cage via π-π tacked interaction.

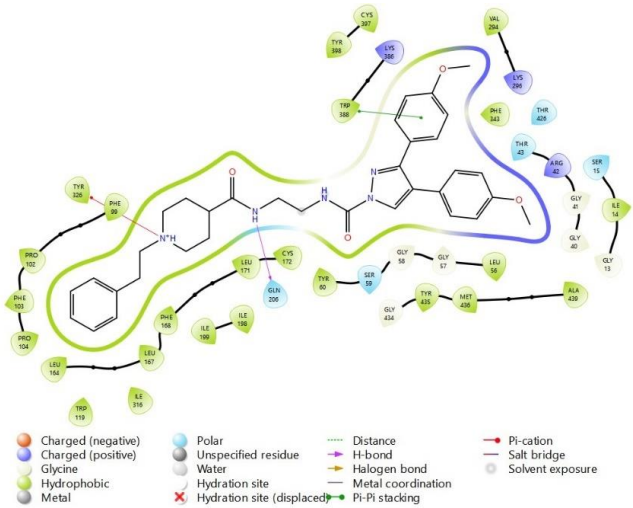

Fig. 4.3: 2D interactions of compound **D2** with MAO-B (PDB Id- 2V5Z).

Similarly, **Fig. 4.3** shows the interaction of compound **D2** with active site of MAO-B. NH of benzyl piperidine interacted with bridge of the substrate cavity amino acid Tyr326 via H-bond interaction along with a H-bond interaction with Gln206 by NH of amide and vicinal

diaryl pyrazole moiety entered in the substrate site and interacted with and phenyl ring interacted with amino acid Trp388 and Tyr398 of aromatic cage via π-π tacked interaction.

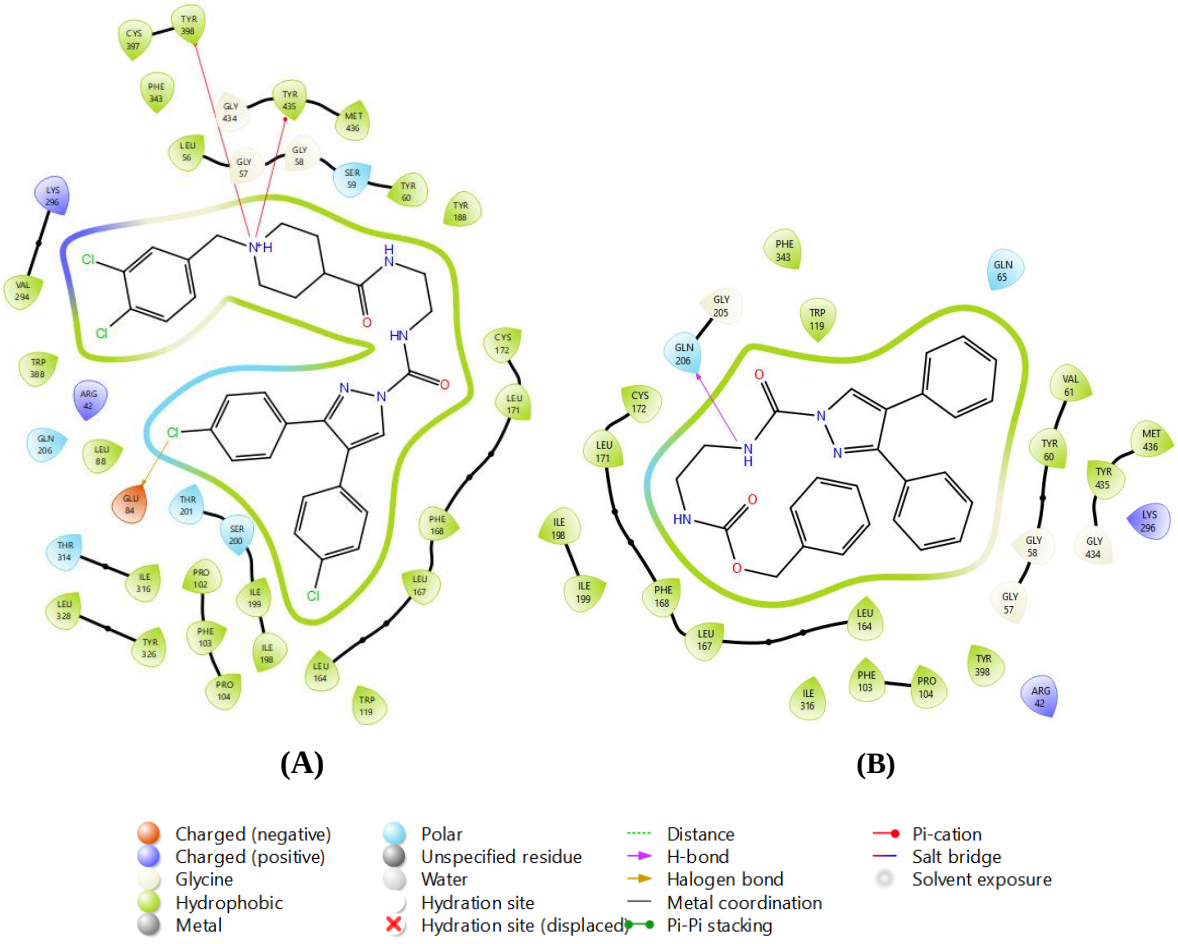

Fig. 4.4: 2D interactions of compound **D3(A)** and **D4 (B)** with MAO-B (PDB Id- 2V5Z).

In compound **D3** (**Fig. 4.4A**), It fitted into the substrate binding pocket where pyrazole of diphenyl pyrazole moiety interacted with Tyr398 via π-π tacked interaction of oxygen and NH of amide linked with benzyl piperidine interacted with Tyr435 and Leu171 via H-bond, respectively. Compound **D4** was chosen as a typical ligand based on inhibitory results. **Fig. 4.4B**, showed that compound **D4** was found in both the substrate and entry cavity of the binding pocket of *h*MAO-B. NH of urea moiety interacted through hydrogen bond with Gln206. Active site amino acids such as Ile199, Cys172, Tyr326, Tyr398 and Tyr435 were interacted through hydrophobic interactions.

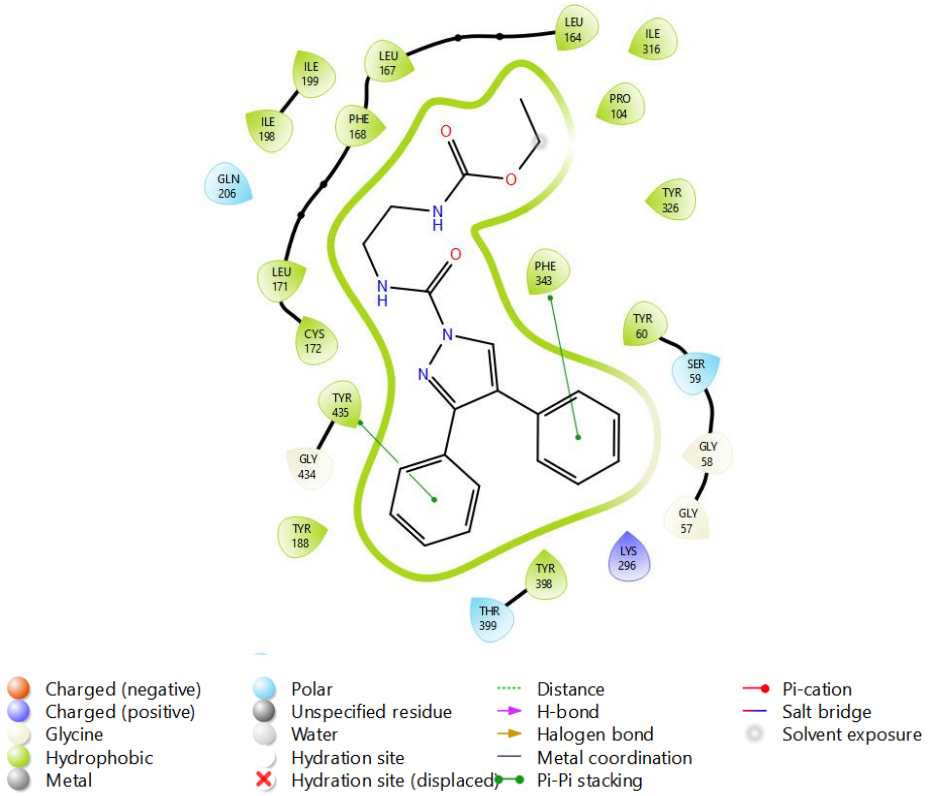

Fig. 4.5: 2D interactions of compound **D5** with MAO-B (PDB Id- 2V5Z).

Compound **D5** (**Fig. 4.5**) was interacting with Tyr188, Lys296 and Tyr398. Other key amino acid of active site such as Ile199, Gln206 and Tyr435 which were in van der waals interaction. 4-methoxyphenyl ring formed H-bond with Lys296 and Pyrazole moiety interacted with Tyr398 through π-π stacking interaction. Whereas Oxygen of urea moiety of the compound **D5** interacted with Tyr188 via H-band. **D5** had lack of key active site amino acid interaction of MAO-B could affect its activity towards it. Lastly, in the case of compound **D6** which is the most designed compounds amongst interacted well with substrate cavity of active site where pyrazole moiety and phenyl ring interacted with Tyr398 via π-π stacking interaction. On the other hand, NH of urea derivative of compound **D6** form polar hydrophobic interaction with Gln206 via H-bond interactions, respectively.

Compound **D1-D6** interacted CAS and PAS active site of *h*AChE. Where NH group of piperidine and carboxamide of Compound **D1** (**Fig. 4.6A**) formed a hydrogen bond with Trp86 and Trp286 via a π- cation interaction, respectively. Thus, it holds the **D1** into the both active sites very well. Oxygen of urea moiety interacted well with Phe295 via H-bond. Moreover, the pyrazole ring of the diphenyl pyrazole moiety exhibits a π-π stacked interaction with Trp286 in PAS site. In compound **D2** (**Fig. 4.6B**), NH- of benzyl piperidine interacted with Tyr341, Tyr337 and Asp74 via π-cation interactions. Oxygen of amide of

benzyl piperidine moiety interacted with Phe295 via H-bond. Moreover, NH of urea moiety exhibited H-bond with Tyr341. Key amino acid of AChE Trp286 and Trp86 were in hydrophobic interaction with **D2**. Compound **D3** interacted with AChE enzyme (**Fig. 4.6C**). In **D3,** NH- of benzyl piperidine allows for a more heightened π-cation interaction with Tyr337 and Trp86 in CAS site. Phe295 was interacted via H-bond with Oxygen of urea moiety. Moreover, the pyrazole ring of the diphenyl pyrazole moiety exhibits a π-π stacked interaction with Trp286 in PAS site.

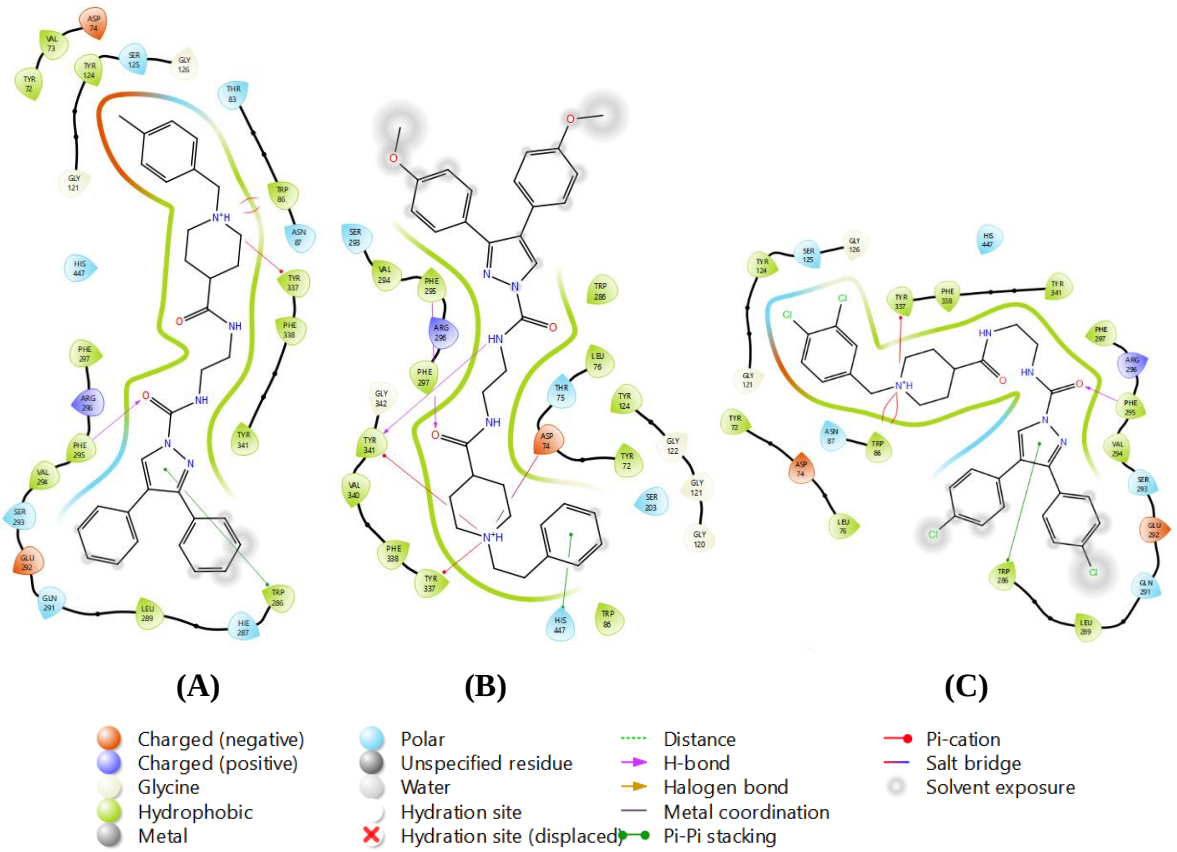

Fig. 4.6: 2D interactions of compound **D1 (A)**, **D2 (B)** and **D3 (C)** with AChE (PDB Id-4EY7).

Compound **D4** had favourable interaction with Trp86 and Trp286 which are key amino acids of binding pocket of the *h*AChE enzyme. (**Fig. 4.7A**) It is oriented along the active site cleft similarly to the reference compound donepezil, stretching from the active site amino acid residue Trp86 to the peripheral site amino acid residue Trp286. The dual binding site inhibitors' significant inhibitory impact is dependent on ligand interactions with these two amino acids. Benzyl carbamate allows for a better π-π stacking interaction with Trp86. In addition, the diphenyl pyrazole ring exhibited π-π stacked with Trp286. Similarly, Pyrazole of compound **D5** also interacted with Trp286, PAS site of active site. Whereas Phenyl ring

formed π-π stacked interactions with Tyr72. Furthermore, oxygen atom from urea moiety interacted with Phe295 through hydrogen bonding. Compound **D5** was interacted with CAS site active amino acid such as Trp86, Tyr337, Phe338 and His447 so on (**Fig. 4.7B**).

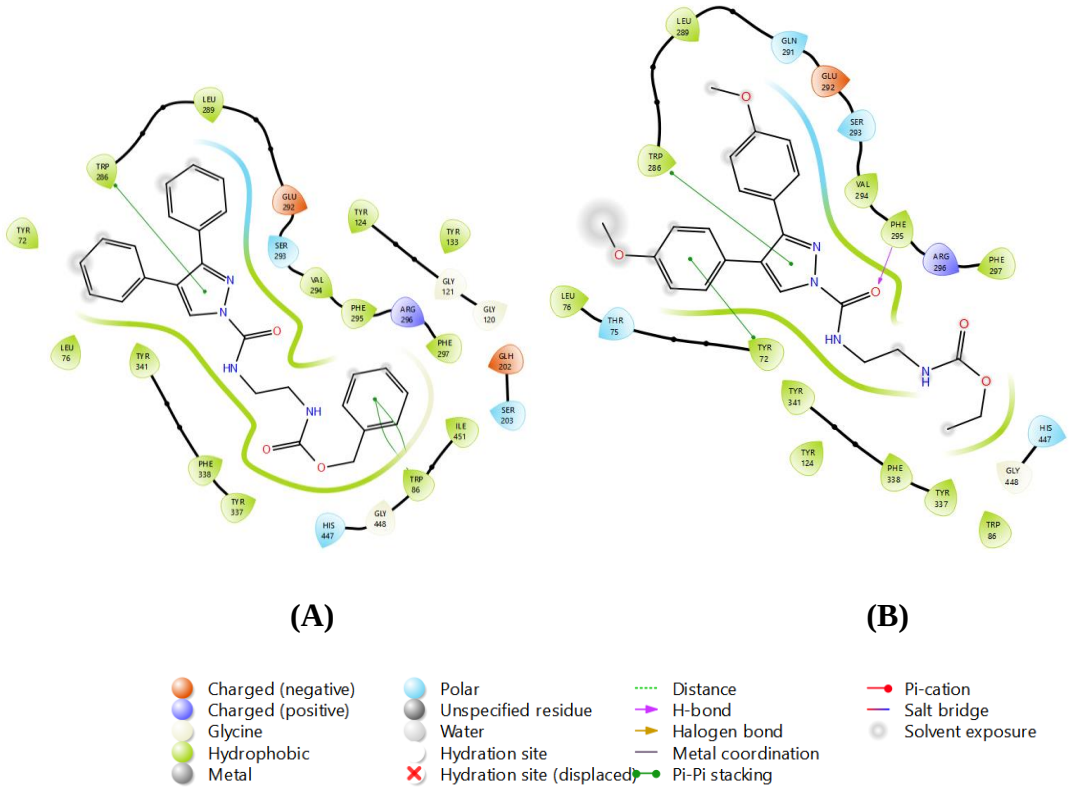

Fig. 4.7: 2D interactions of compound **D4 (A)** and **D5 (B)** with AChE (PDB Id- 4EY7).

Lastly in case of compound **D6** (**Fig. 4.8**), the aromatic ring of benzyl carbamate enables a more enhanced π-π stacking interaction with Trp86 in CAS site. Additionally, pyrazole ring demonstrates π-π stacked interactions with Trp286. Furthermore, Ser293 forms halogen bond interactions with 4-chloro substitution of the diphenyl pyrazole moiety in PAS site.

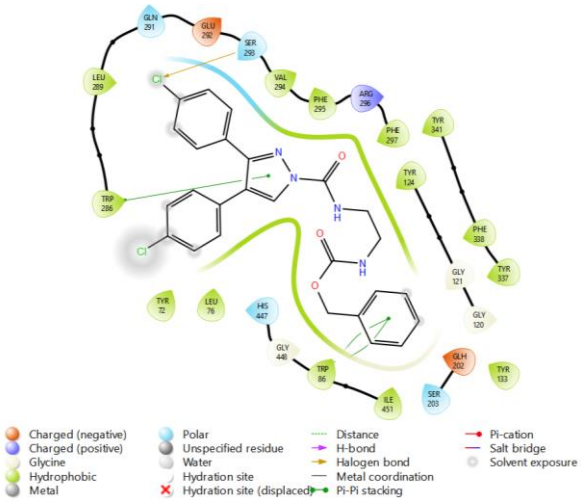

Fig. 4.8: 2D interactions of compound **D6** with AChE (PDB Id- 4EY7).

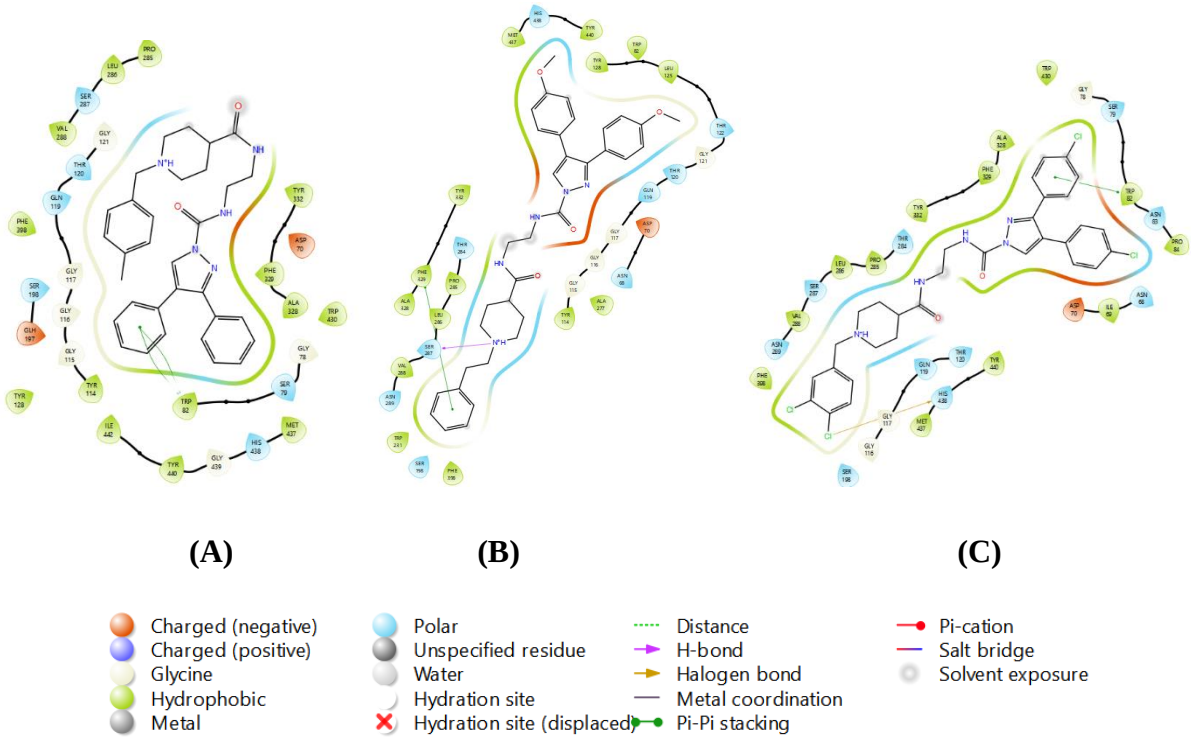

Fig. 4.9: 2D interactions of compound **D1 (A), D2 (B)** and **D3 (C)** with BuChE (PDB Id- 5K5E).

Fig. 4.9A demonstrated that the compound **D1** lined the vast catalytic cavity of BuChE due to its binding structure. The aromatic ring of the diphenyl pyrazole moiety interacted with Trp82 via π-π interaction. Moreover, it interacted with Phe329, Tyr332 and His438 through van-dar waals interactions, respectively. In **D2,** Aromatic ring of benzyl ethyl piperidine moiety and NH- of piperidine formed π-π stacked and hydrogen bond with Phe329 and Ser287, respectively (**Fig. 4.9B**). Finally, compound **D3 (Fig. 4.9C)** occupied the expansive catalytic cavity of BuChE by virtue of its binding structure. The phenyl ring of the

dichloro diphenyl pyrazole moiety of compound **D3** engaged in π-π stacked interaction with Trp82. Additionally, Cl of 3,4-dichloro benzyl piperidine interacted with His438 via halogen bond.

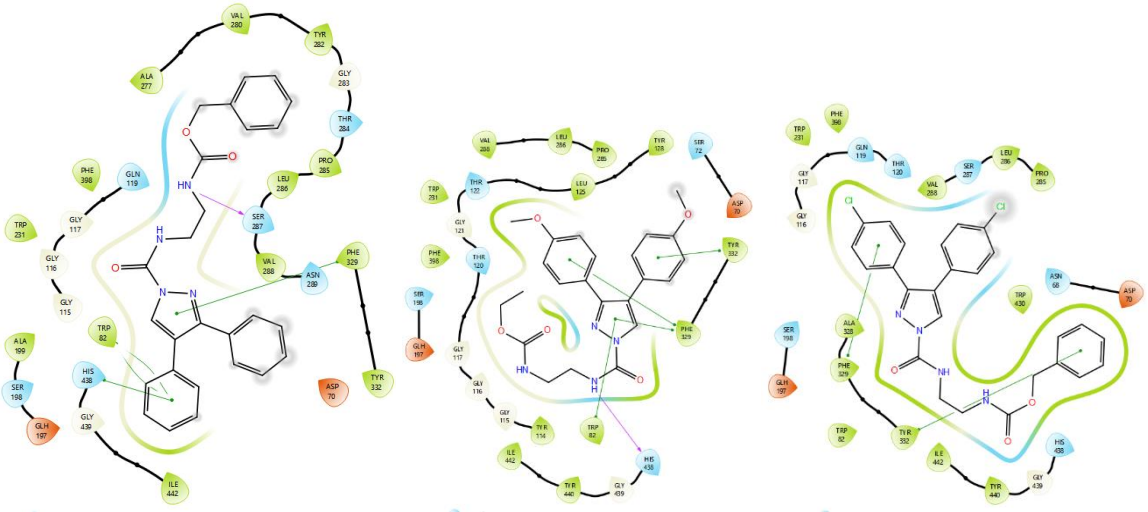

(A) **(B)** **(C)**

Fig. 4.10: 2D interactions of compound **D4 (A), D5 (B)** and **D6 (C)** with BuChE (PDB Id-5K5E).

In **Fig. 4.10A** demonstrated that the compound **D4** lined the vast catalytic cavity of BuChE due to its binding structure. Pyrazole moiety interacts with Trp82 via π-π stacked interaction. The aromatic ring of the diphenyl pyrazole moiety interacted with Phe329, and His438 via a π-π t-shaped contact. Secondly amine of benzyl carbamate interacted through Ser287 via H-bonding. In compound **D5** (**Fig. 4.10B**), the diphenyl pyrazole moiety's aromatic ring engaged in a π-π interaction with Phe329 and Tyr332. Pyrazole moiety established π-π stacked interactions with Trp82 and Phe329. His438 also formed interactions with amine of urea moiety through a hydrogen bond. Lastly, the aromatic ring of the diphenyl pyrazole moiety of compound **D6** also interacted with Phe329 via π-π tacked interaction and benzyl ring of carbamate moiety formed π-π stacked interaction with Tyr332 (**Fig. 4.10C**).

4.1.1. *In-silico* physicochemical and pharmacokinetic descriptors prediction of pyrazole-based compounds

ADME prediction was performed for the designed compounds among of them most active compound **D1-D5** discussed elaborately **(Table 4.3)**. Donepezil, Rivastigmine and Safinamide were taken as reference drugs. Physicochemical and pharmacokinetic profiling of designed molecule and reference drugs were based on descriptors such as QlogPo/w, QlogS,

QlogBB, QPPMDCK, QPlogKhsa, SASA, % oral absorption, PSA, Lipinski rule of Five. (Cite) Lipinski rule of five (RO5) give parameters for druglikeliness of compounds. As per it for drug likeliness molecules should have ≤ 500 molecular weight, ≤ 5 Log P value, ≤ 5 HBD (Hydrogen Bond Donor) and ≤ 10 HBA (Hydrogen Bond Acceptor).[2] As per the **Table 4.3** except compound **D4** all were violating the rule of five. Violation of more than one among them suggests poor absorption or permeation thus it predicts that except **D4** all might have absorption and permeability issues. **D5**, the only molecule having molecular weight under 500 other, 3 compounds have violated it. Secondly, All the compounds having HBD below 5 and HBA below 10. The key descriptors for the CNS active drugs which can predict permeation of BBB are Brain/blood partition coefficient (QPlogBB), n-octanol−water partition coefficient (QPlogPo/w), apparent MDCK cell permeability (QPPMDCK), and CNS. n-octanol-water partition coefficient (QPlogPo/w) value should be in the range of -2 to 6.5 but for optimum value for penetration of molecule from BBB passively should be around 3.[3]

Table 4.3: QikProp physicochemical and pharmacokinetic descriptors for compound (**D1-D5)** respectively.

Descriptors	Range	D1	D2	D3	D4	D5	Donepezil	Rivastigmine	Safinamide
Rule of 5	0−1	2	1	2	0	2	0	0	0
MW	130−725	521.661	581.713	645.414	438.482	509.391	379.498	250.34	300.332
HBD	0−6	2	2	2	2	2	5.5	0	2
HBA	2−20	7.5	9	7.5	7	5.5	0	5	2
QPlogPo/w	−2 to 6.5	5.162	4.502	6.019	3.877	6.178	4.242	2.287	2.759

QPlogBB	−3 to 1.2	-0.489	-0.475	0.279	-0.904	-0.776	0.223	0.349	-0.865
QPPMDCK	<25 poor, >500 great	199.077	184.428	5311.603	500.028	2406.726	589.289	538.056	816.96
QPlogKhsa	−1.5 to 1.5	0.882	0.554	0.936	0.403	1.106	0.516	-0.163	-0.176
CNS	-2 to +2	1	1	1	-1	-1	1	1	-1
%Human Oral Absorption	0−100	72.457	79.2	75.937	100	85.979	100	93.906	90.753
PSA	7 to 200	119.298	113.106	114.547	97.891	119.62	46.234	39.092	69.111
#Star	0 – 5	4	1	3	0	4	0	0	0

Rule of 5: Lipinski Rule of 5; MW: Molecular Weight; HBD: Hydrogen Bond Donor; HBA: Hydrogen Bond Acceptor; QPlogPo/w: predicted octanol/water partition coefficient; QPlogBB: brain/blood partition coefficient; QPPMDCK: predicted apparent MDCK cell permeability in nm/s; QPlogKhsa: binding to human serum albumin; CNS: predicted central nervous system activity on a −2 (inactive) to +2 (active) scale; % Human Oral Absorption; PSA: Polar Surface area; #Star: number of parameters with values that fall outside the 95% range of similar values for known drugs.

QPlogBB predicts brain/blood partition coefficient where all the compounds were having negative except **D3** which indicated that the compound is too polar to cross BBB. QPlogBB. QPPMDCK predicts MDCK cell permeability in nm/s. MDCK is to be good mimic for the BBB which is for non-active transports. >25 value of QPPMDCK is considered to be good and all the compounds have high value.[4] Compounds **D4**, **D5**, and **D3** were above 500 value where considered as a great for the non-active permeation. CNS descriptor predicts CNS activity on the scale of -2 (inactive) to 2 (active) **D4** and **D5** weakly active; and **D1, D2,** and **D3** are active as they having positive CNS values. QPlogKhsa predicts CNS active drugs binding with human serum albumin where all the compounds were predicted as having low binding with it and unbound drug bind with receptor for activity.[5] % Human Oral Absorption

(%HOA) was also predicted that all the compounds may have oral bioavailability. Polar surface area and rotatable bonds are the most important descriptors.[6] Rotatable bonds are for the information of flexibility and helps to predict the oral bioavailability of compounds. It should be less than 7 or 8 rotatable bonds. PSA predicts polar diffusion of molecule through membrane which helps to predict drug intestinal absorption, bioavailability and BBB prediction. It should be in the range of 4.63−108 Å^2.[7,8] All the test compounds rotatable bonds in the range of 5-9 and PSA is also in well-defined range. QPCaco-2 predicts the permeation of drug from Caco-2 cell membrane which gives gut-blood brain barrier partition coefficient. It predicts oral bioavailability of drug.[9] It was predicted that all the test compounds were able to permeate effectively from Caco-2 cell membrane. #Star indicates number of descriptors fall outside the range of drug likeliness. Larger the number lesser the drug likeliness of the molecules. Compound **D5** and **D3** had less drug likeliness as it had 4, 4 and 3 #stars, respectively. On the other hand, **D4** had high drug likeliness as it had 0 and 1 #stars, respectively. Thus, it indicated that among six designed compounds, **D4** had more drug likeliness than others.

4.2. *In silico* studies of benzofuran-based compounds

All designed compounds were docked and analyzed by the binding energies and receptor ligand interactions. The interactions of compounds which had the highest docking score compare to standards within active site of *h*MAO-B are discussed here in detail **(Table 4.4)**.

Table. 4.4: Docking score and interactions of compound **(D7-D9)** against *h*MAO-B (PDB: 2V5Z).

Code	Compound	*h*MAO-B (PDB: 2V5Z)		
		Docking Score (Kcal/Mol)	Interactions	Type of Interaction
D7	**182**	-11.89	Gln206 Trp388 Tyr398	H-bond π-π stacking π-π stacking
D8	**183**	-12.22	Gln206 Trp388 Tyr398	H-bond π-π stacking π-π stacking
D9	**188**	-12.31	Gln206 Tyr398 Tyr435	H-bond π-π stacking π-π stacking
	Safinamide	-11.18	Gln206 Tyr326	H-bond π-π stacking

Grid validation was performed by redocking of co-crystalized molecules in 3D protein structures of *h*MAO-B (PDB: 2V5Z) active site. Initially, co-crystallized ligands were extracted from the binding site. This extracted co-crystalized ligand were energy minimized and redocked into the active site. **Fig. 4.11.** shows the RMSD value of redocked ligands with co-crystallized ligands in 2V5Z was observed which was 0.14, respectively.

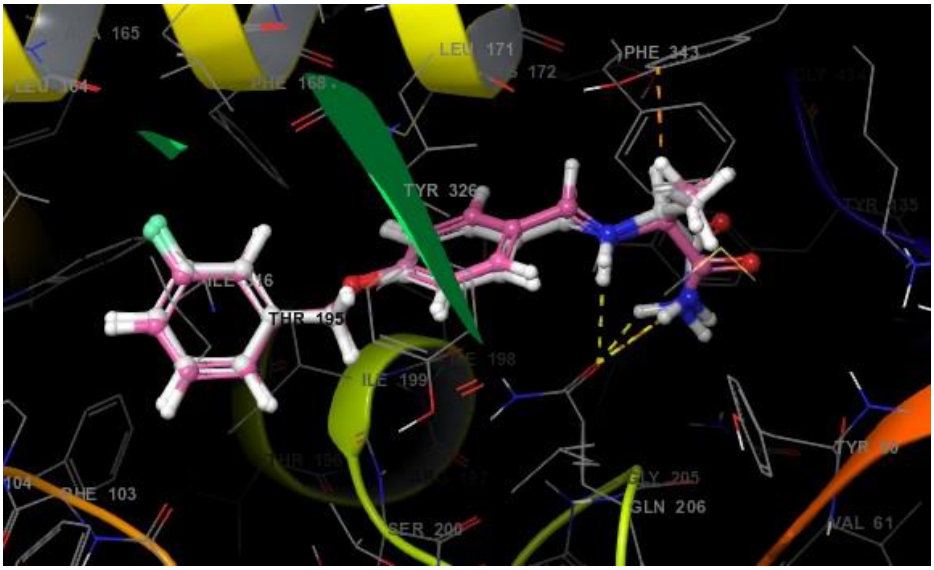

Fig. 4.11: Aligned redocked ligands (pink) with co-crystallized ligand (white) for 2V5Z.

The bipartite MAO-B active site consists of two cavities: an entry cavity and a substrate cavity with an aromatic cage. Here safinamide is co-crystallized ligand having docking score of -11.178 Kcal/Mole. **Fig. 4.12.** shows that benzyloxy moiety of the safinamide interact with Tyr326 through π-π stacking interactions and NH of schiff base and amide interacted with Gln206 through hydrogen bonding. This suggests that to have good MAO-B inhibition Tyr326 and Gln206 are the key amino acids. Thus, during designing lead molecules for the MAO-B inhibition there should be interaction of these two amino acids.

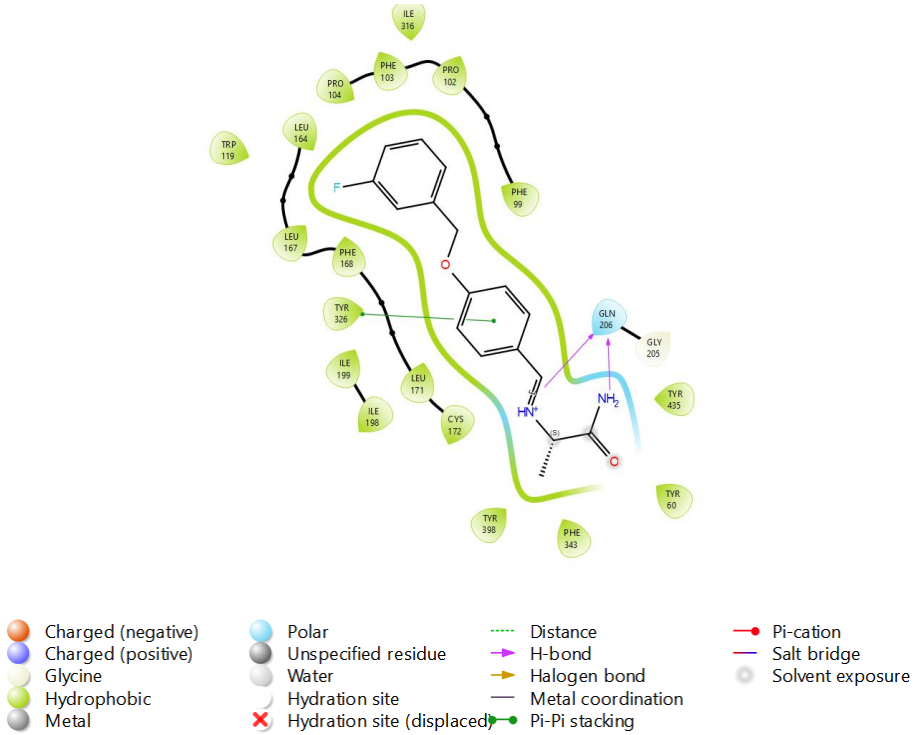

Fig. 4.12: 2D interaction of safinamide with active of MAO-B (PDB id- 2V5Z).

Here, among of all designed compounds compound **D7, D8** and **D9** are discussed elaborately. They interacted with Pro102, Ile199 and Tyr326 which are key amino acids of entrance cavity, besides that they also interacted with substrate cavity key amino acids such as Phe343, Trp388, Tyr398, Tyr435 and Met436. **Fig. 4.13.** showed 2D interactions of compound **D7**. The docking score of this compound is better than the co-crystalized ligand safinamide which is -11.89 Kcal/mole. Compound **D7** was well interacted with entrance cavity and substrate cavity of active site of MAO-B where NH of benzamide interacted with Gln206 via hydrogen bonding. Aromatic ring of benzofuran moiety and furan of furfuraldehyde interacted with substrate cavity amino acids Tyr398 and Trp388 through π-π stacking interaction, respectively.

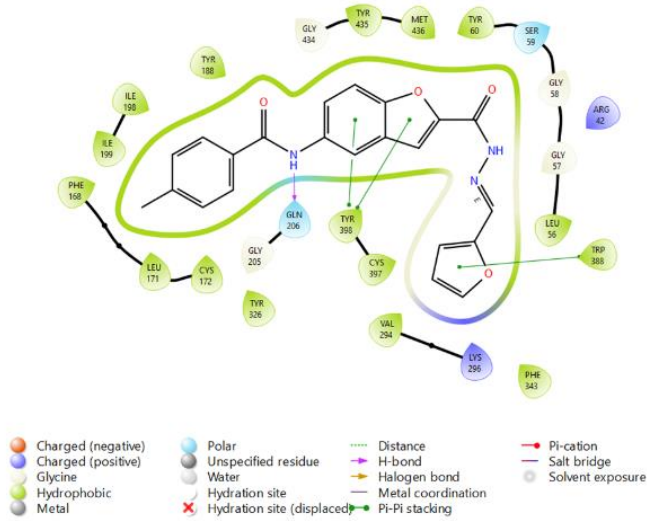

Fig. 4.13: 2D interactions of compound **D7** with MAO-B (PDB Id- 2V5Z)

2D interaction of compound **D8 (Fig. 4.14.)** suggests that it interacted well with entrance cavity and substrate cavity with docking score -12.218 Kcal/mole which is also better than the safinamide. It had somewhat similar docking interaction as it had hydrogen bond interaction between Gln206 and NH of benzamide. Similarly to the compound **D8** benzofuran moiety was also interacted well with Tyr398 via π-π stacking. Lastly thiophene ring of schiff base of thiophene-2-carbaldehyde interacted alike benzofuran moiety with Trp388 via π-π stacking.

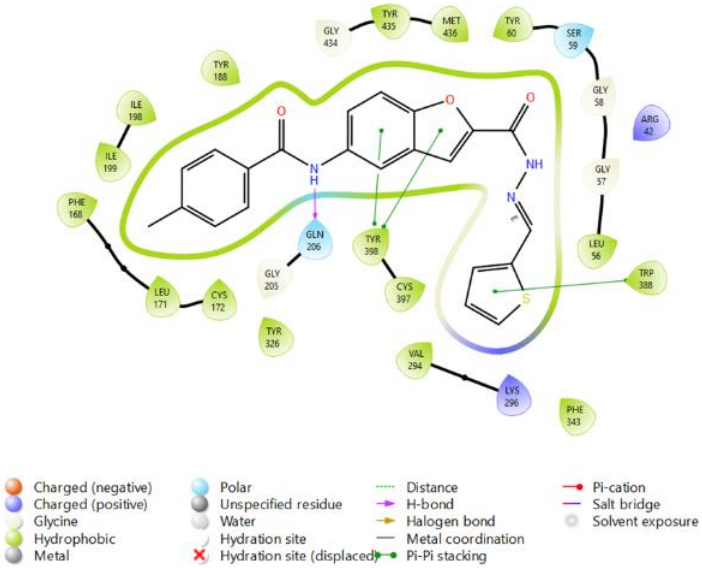

Fig. 4.14: 2D interactions of compound **D8** with MAO-B (PDB Id- 2V5Z)

Fig. 4.15 suggested that compound **D9** had good affinity with the substrate and entrance cavity of active site amino acid of MAO-B. As per the affinity result data, it had very good affinity with active site as it had docking score (-12.314 Kcal/mole) higher than the safinamide. 2D interactions of this compound showed that the NH of benzamide was interacted well with key substrate cavity polar amino acid which is Gln206 via hydrogen bonding. Tyr398 and Tyr435 amino acid of aromatic cage of substrate cavity tightly interacted with benzofuran moiety via π-π stacking interaction. Lastly, benzene ring of schiff base derivative of benzaldehyde interacted nicely with Tyr388 via π-π stacking.

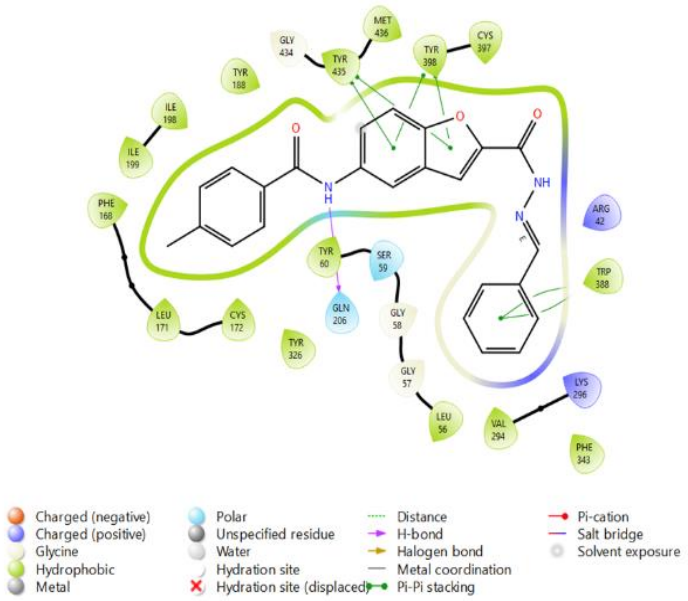

Fig. 4.15: 2D interactions of compound **D9** with MAO-B (PDB Id- 2V5Z)

4.2.1. *In-silico* physicochemical and pharmacokinetic descriptors prediction of benzofuran-based compounds

ADME prediction was performed for all the designed compounds and discussed elaborately with respect to safinamide which was taken as reference drug. (**Table 4.5**) Physicochemical and pharmacokinetic profiling of designed molecule and reference drugs were based on descriptors such as QlogPo/w, QlogS, QlogBB, QPPMDCK, QPlogKhsa, SASA, % oral absorption, PSA, Lipinski rule of Five. Lipinski rule of five (RO5) give parameters for druglikeliness of compounds. As per it for drug likeliness, molecules should have ≤ 500 molecular weight, ≤ 5 LogP value, ≤ 5 HBD (Hydrogen Bond Donor) and ≤ 10 HBA (Hydrogen Bond Acceptor).[2] **D12** and **D13** were following RO5. All the compounds having HBD below 5 and HBA below 10. The key descriptors for the CNS active drugs which can predict permeation of BBB are Brain/blood partition coefficient (QPlogBB), n-

octanol−water partition coefficient (QPlogPo/w) and apparent MDCK cell permeability (QPPMDCK). n-octanol-water partition coefficient (QPlogPo/w) value should be in the range of -2 to 6.5 but for optimum value for penetration of molecule from BBB passively should be around 3.[3] All the designed compounds were having QPlogPo/w value in range except. Secondly, they had QPlogPo/w value above the standard safinamide which was 2.759. QPlogBB predicts brain/blood partition coefficient where all the compounds were having negative which indicated that all the compounds were well enough to cross BBB.

Table 4.5: QikProp physicochemical and pharmacokinetic descriptors for compound **D7-D9.**

Code	RO5[a]	HBD[b]	HBA[c]	QPlogPo/w[d]	QPlogBB[e]	QPPMDCK[f]	QPlogKhsa[g]	%HOA[h]	QPPCaco[i]
D7	0	2	6	3.962	-1.195	303.131	0.453	100	635.62
D8	0	2	5.5	4.578	-1.092	573.681	0.644	100	651.44
D9	0	2	5.5	4.652	-1.217	314.95	0.719	100	658.51
Safinamide	0	2	2	2.759	-0.865	816.96	-0.176	90.75	459.71

[a]RO5: Lipinski Rule of 5 (0-1); [b]HBD: Hydrogen Bond Donor **(0-6)**; [c]HBA: Hydrogen Bond Acceptor **(2-20)**; [d]QPlogPo/w: predicted octanol/water partition coefficient **(−2 to 6.5)**; [e]QPlogBB: brain/blood partition coefficient **(-3 to 1.2)**; [f]QPPMDCK: predicted apparent MDCK cell permeability in nm/s **(<25 poor, >500 great)**; [g]QPlogKhsa: binding to human serum albumin **(-1.5 to 1.5)**; [h]%HOA: % Human Oral Absorption **(0-100)**; [i]QPPCaco: Predicted apparent Caco-2 cell permeability in nm/sec **(<25 poor, >500 great).**

Compare to standard safinamide all the compounds have high QPlogBB. MDCK is to be good mimic for the BBB which is for non-active transports. >25 value of QPPMDCK is considered to be good and all the compounds have high value.[4] All the compounds had values above 25 as they had good non-active permeability. Compounds **D7** and **D8** had the MDCK value above 500 which indicated that they were predicted as having great non-active BBB transport. QPlogKhsa predicts CNS active drugs binding with human serum albumin where all the compounds were predicted as having high binding with it and less unbound drug bind with receptor for activity[5] with respect to safinamide (QPlogKhsa value: -0.176). % Human Oral Absorption (%HOA)[6] was also predicted that all the compounds may have oral bioavailability. QPCaco-2 predicts the permeation of drug from Caco-2 cell membrane which gives gut-blood brain barrier partition coefficient. It predicts oral bioavailability of drug. It was predicted that all the test compounds were able to permeate effectively from Caco-2 cell membrane.[7–9]

4.2.2. Molecular docking studies of compounds (D10 - D13)

Docking studies were carried out in Autodock vina 1.5.6 to see the binding interactions of the designed compounds in the active site along with standard rivastigmine for **D10** and **D11.**

Table 4.6: Binding affinity score of compounds **D10** and **D11** on AChE and BuChE enzymes

Code	Compound	AChE Binding affinity (Kcal/mol)	BuChE Binding affinity (Kcal/mol)
D10	**203**	**-11.4**	**-9.6**
D11	**212**	**-11.3**	**-9.8**
	Rivastigmine	**-7.9**	**-7.1**

Among all the designed compounds showed better binding affinity with AChE enzyme than the standard drug rivastigmine. Compound **D10** and **D11** showed binding affinity **-11.4 Kcal/mol** and **-11.3 Kcal/mol** with AChE enzyme.

Docking studies of rivastigmine with AChE enzyme indicated phenyl ring formed pi-pi stacked bond with Phe338 and Tyr337 along with pi-pi T shaped bond with Tyr341. While carbonyl oxygen of carbamate showed pi-anion bond with Tyr341. Ethyl chain showed pi-alkyl bond with Trp286 and methyl group of tertiary amine showed carbon hydrogen bond with Ser203. Interaction of rivastigmine with AChE active site is shown in **Fig. 4.16**.

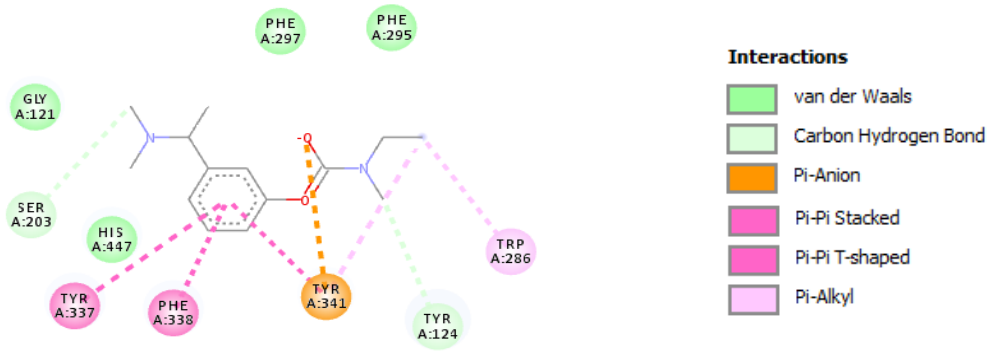

Fig. 4.16: Interaction of rivastigmine with AChE (PDB: 4EY7).

Docking studies of compound **D10** with AChE enzyme indicated phenyl ring formed pi-pi stacked bond with His447 and Trp86. While benzofuran ring showed pi-pi T shaped bond with Ser293 along with pi-Alkyl bond with Val294. Also, phenyl ring between two amide group showed Amide-pi stacked bond with Try337 and Phe338. Carbonyl oxygen of

amide group showed conventional hydrogen bond with Tyr124. Interaction of compound **D10** with AChE active site is shown in **Fig. 4.17**.

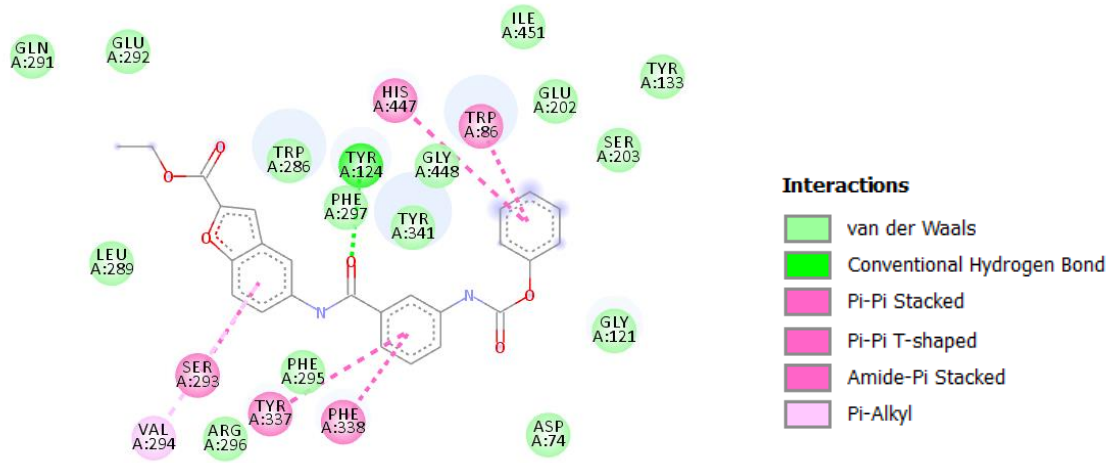

Fig. 4.17: 2D **i**nteraction of compound **(D10)** with AChE (PDB: 4EY7).

Docking studies of compound **D11** with AChE enzyme indicated phenyl ring formed pi-alkyl bond with Val73, Pro88 and Leu92. While benzofuran ring showed pi-anion bond with Glu81 and Asp131 along with pi-alkyl bond with Met85 also ethyl chain showed pi-alkyl bond with Met85 and aromatic ether of benzofuran ring showed conventional hydrogen bond with Arg463. Interaction of compound **D11** with AChE active site is shown in **Fig. 4.18**.

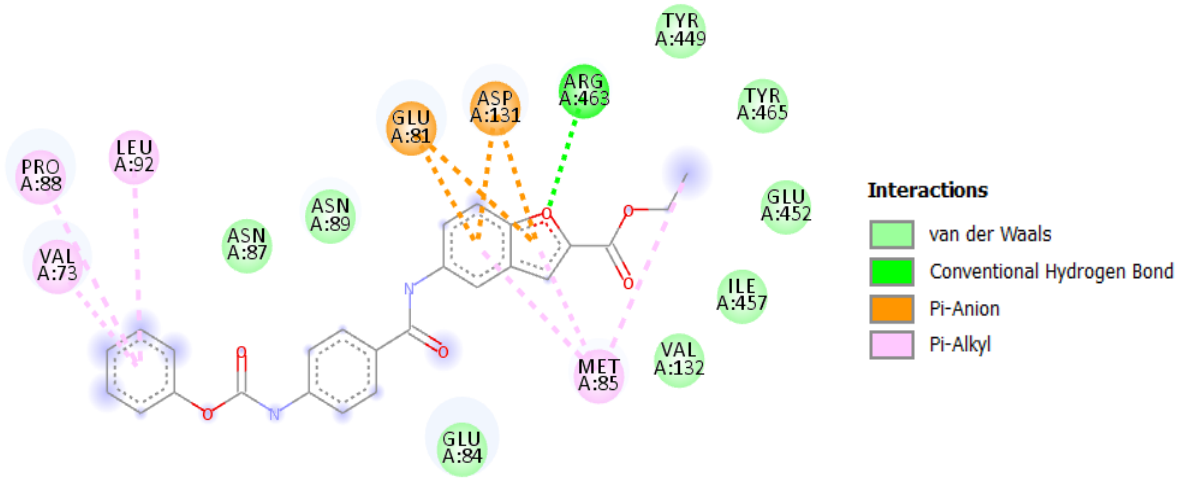

Fig. 4.18: 2D interactions of compound **(D11)** with AChE (PDB: 4EY7).

4.2.3. Molecular docking studies of compounds (D12 and D13)

Compounds **D12** and **D13** were docked with MAO-B PDB:2V5Z and 2D interactions are described in detail **(Table 4.7)**.

Table 4.7: Binding affinity of compounds **(D12** and **D13)** with MAO-B PDB:2V5Z

Code	Compound	Docking score	Interactions	Type of Interaction
D12	**223**	-12.17	Ser59 Tyr398 Tyr326 Trp388	H-Bond π-π stacking π-π stacking π-π stacking
D13	**224**	-11.85	Trp388 Tyr435 Tyr398 Tyr326	π-π stacking π-π stacking π-π stacking π-π stacking
	Safinamide	-11.18	Gln206 Tyr326	H-bond π-π stacking

Compound **(D12)** interacted with entrance cavity and substrate cavity of active site of MAO-B wherein the carbonyl oxygen of amide interacted via hydrogen bonding with Ser59. Aromatic ring of benzofuran moiety interacted with substrate cavity amino acids Tyr326, Tyr398 and Trp388 through π-π stacking interaction, respectively **(Fig. 4.19).**

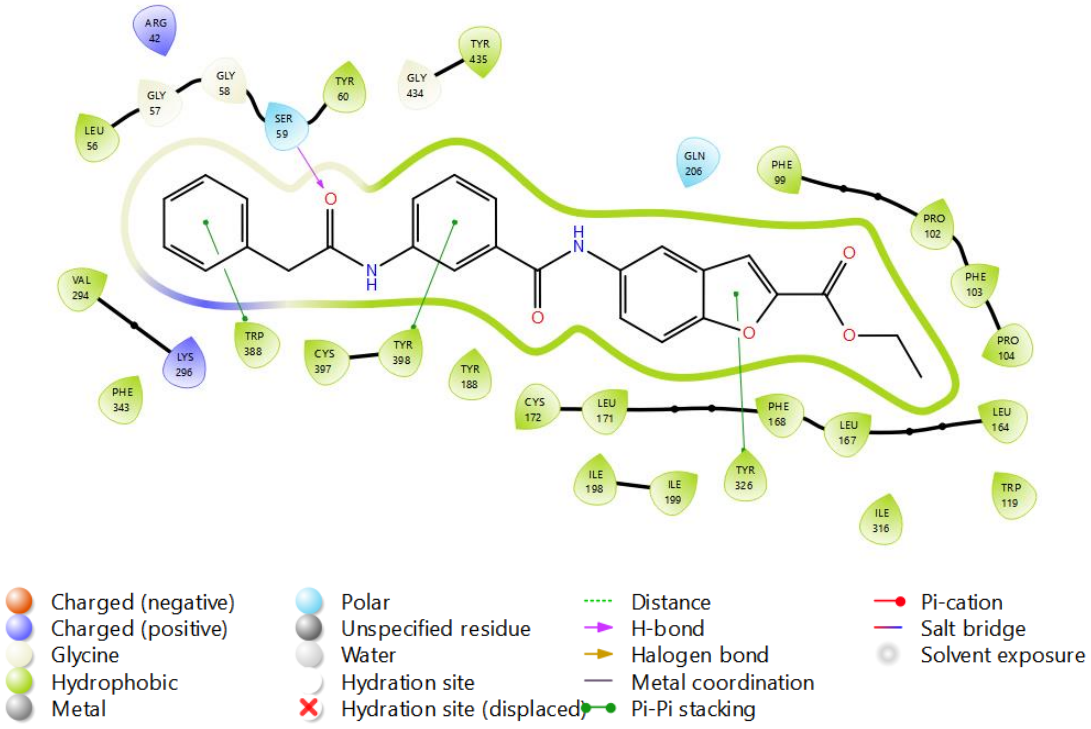

Fig. 4.19: 2D interactions of compound **(D12)** with MAO-B (PDB Id- 2V5Z).

Compound **D13 (Fig. 4.20)** suggests that it interacted well with entrance cavity and substrate cavity with docking score -11.78 Kcal/mol higher than safinamide. Pyridine ring produced intreaction with Trp388 via π-π stacking while benzofuran moiety interacted with

Tyr326 which is a crucial amino acid of the bridge in the substrate cavity along another key interaction produced by benzene ring with Tyr398 and Tyr435.

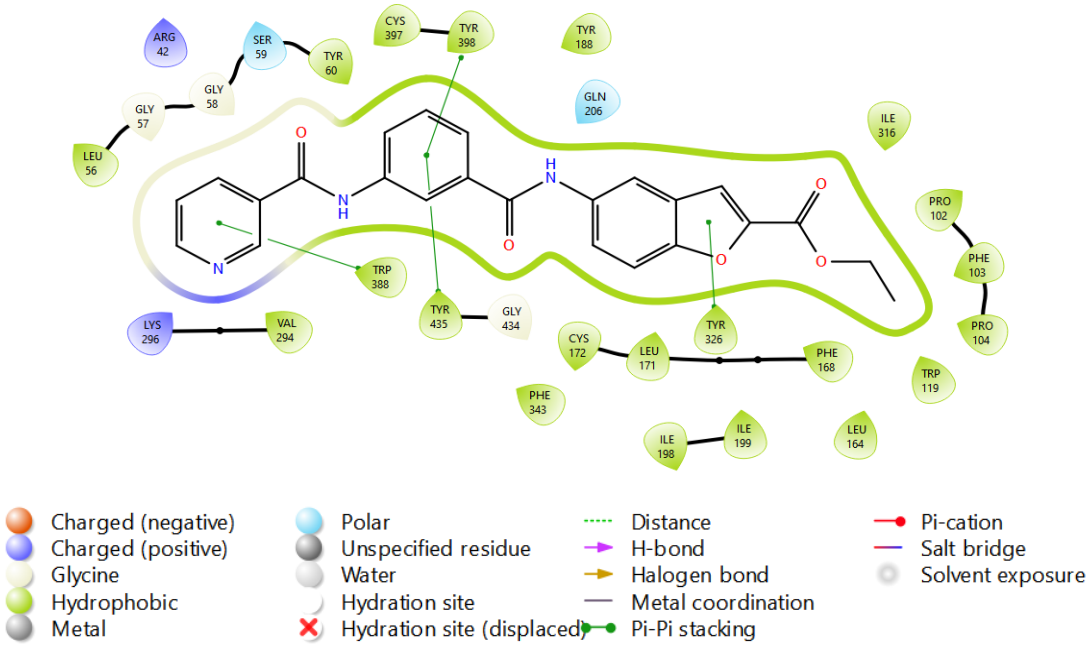

Fig. 4.20: 2D interactions of compound **(D13)** with MAO-B (PDB Id- 2V5Z).

4.2.4. ADME predictions of compounds (D12-D13)

ADME prediction was done for all the designed compounds and the results are described in **(Table 4.18.)** The physicochemical and pharmacokinetic profiles of designed molecules and reference safinamide are based on descriptors such as QlogPo/w, QlogS, QlogBB, QPPMDCK, QPlogKhsa, SASA, % oral absorption, PSA, and the Lipinski rule of five.

Table 4.18: Physicochemical properties of compounds **(D12-D13).**

Code	RO 5[a]	HB D[b]	HB A[c]	QPlogPo/ w[d]	QPlogB B[e]	QPPMDC K[f]	QPlogKhs a[g]	%HO A[h]	QPPCac o[i]
223	0	2	7.5	4.448	-1.85	130.517	0.67	100	291.486
224	0	2	9	3.242	-2.03	76.717	0.253	86.22	178.285

[a]RO5: Lipinski rule of 5 **(0-1)**; [b]HBD: Hydrogen bond donor **(0-6)**; [c]HBA: Hydrogen bond acceptor **(2-20)**; [d]QPlogPo/w: predicted octanol/water partition coefficient **(−2 to 6.5)**; [e]QPlogBB: brain/blood partition coefficient **(-3 to 1.2)**; [f]QPPMDCK: predicted apparent MDCK cell permeability in nm/s **(<25 poor, >500 great)**; [g]QPlogKhsa: binding to human serum albumin **(-1.5 to 1.5)**; [h]%HOA: % Human oral absorption **(0-100)**; [i]QPPCaco: Predicted apparent Caco-2 cell permeability in nm/sec **(<25 poor, >500 great).**

D12 and **D13**, followed RO5. Furthermore, all the designed compounds have total HBD below 5 and total HBA below 10. QPlogPo/w value determines octanol/water partition coefficient. For the compounds **D12** and **D13,** QPlogPo/w value was predicted to be above

the standard safinamide i.e. 2.759. It indicates that the compounds are more hydrophobic compared to safinamide. QPlogBB predicts brain/blood partition coefficient. For all the designed compounds QPlogBB predicted to be negative indicating that the compounds are lipophilic enough to cross BBB. Compared to standard safinamide, all the compounds predicted to be having lower QPlogBB value. Compound **D13** predicted to be having lowest QPlogBB value (-2.03).

The anticipated apparent permeability of MDCK cells, measured in nm/s (^{f}QPPMDCK), reflects the ease with which a compound can traverse the cell membrane of MDCK (Madin-Darby Canine Kidney) cells. These cells serve as a widely used model for investigating epithelial transport and permeability. An increased value of fQPPMDCK signifies enhanced permeability, indicating that the molecule is more prone to being taken up by the cell. The value of QPPMDCK (>25) is considered to be good. For the designed compounds, QPPMDCK value was predicted to be higher than 25.[4]

QPlogKhsa refers to a predictive model for binding of molecules to human serum albumin (HSA). It is an indicator of the potential affinity or capacity of a compound to bind to HSA, which can significantly affect the drug's distribution, efficacy, and metabolism in the human body. The designed compounds were predicted to have high binding with it and less unbound drug bind with receptor for activity[5] with respect to safinamide (QPlogKhsa value: -0.176).

After considering the results of molecular docking interactions and physiochemical parameters of designed compounds, the compounds were proposed as anti-AD molecules and planned to synthesize and evaluate for AChE, BuChE and MAO-B enzyme inhibitory activities.

4.3. References

(1) Milczek, E. M.; Binda, C.; Rovida, S.; Mattevi, A.; Edmondson, D. E. The 'Gating'Residues Ile199 and Tyr326 in Human Monoamine Oxidase B Function in Substrate and Inhibitor Recognition. *FEBS J.* **2011**, *278* (24), 4860–4869.

(2) Lipinski, C. A.; Lombardo, F.; Dominy, B. W.; Feeney, P. J. Experimental and Computational Approaches to Estimate Solubility and Permeability in Drug Discovery and Development Settings. *Adv. Drug Deliv. Rev.* **1997**, *23* (1–3), 3–25.

(3) Waterhouse, R. N. Determination of Lipophilicity and Its Use as a Predictor of Blood–Brain Barrier Penetration of Molecular Imaging Agents. *Mol. Imaging Biol.* **2003**, *5* (6), 376–389.

(4) Wang, Q.; Rager, J. D.; Weinstein, K.; Kardos, P. S.; Dobson, G. L.; Li, J.; Hidalgo, I. J. Evaluation of the MDR-MDCK Cell Line as a Permeability Screen for the Blood–Brain Barrier. *Int. J. Pharm.* **2005**, *288* (2), 349–359.

(5) Lexa, K. W.; Dolghih, E.; Jacobson, M. P. A Structure-Based Model for Predicting Serum Albumin Binding. *PLoS One* **2014**, *9* (4), e93323.

(6) Veber, D. F.; Johnson, S. R.; Cheng, H.-Y.; Smith, B. R.; Ward, K. W.; Kopple, K. D. Molecular Properties That Influence the Oral Bioavailability of Drug Candidates. *J. Med. Chem.* **2002**, *45* (12), 2615–2623.

(7) Kelder, J.; Grootenhuis, P. D. J.; Bayada, D. M.; Delbressine, L. P. C.; Ploemen, J.-P. Polar Molecular Surface as a Dominating Determinant for Oral Absorption and Brain Penetration of Drugs. *Pharm. Res.* **1999**, *16*, 1514–1519.

(8) Pajouhesh, H.; Lenz, G. R. Medicinal Chemical Properties of Successful Central Nervous System Drugs. *NeuroRx* **2005**, *2*, 541–553.

(9) Chan, E. C. Y.; Tan, W. L.; Ho, P. C.; Fang, L. J. Modeling Caco-2 Permeability of Drugs Using Immobilized Artificial Membrane Chromatography and Physicochemical Descriptors. *J. Chromatogr. A* **2005**, *1072* (2), 159–168.

***